

Innovative Determination of Zinc Isotope Ratios in Geological Reference Materials: A Combined Precipitation and Anion Exchange Resin Method by MC-ICP-MS

Xiaojuan Nie, Zhian Bao, Chunlei Zong, Deyi Peng, Nan Lv, and Honglin Yuan*

State Key Laboratory of Continental Dynamics, Department of Geology, Northwest University, Xi'an 710069, P. R. China

Received: June 18, 2024; Revised: August 29, 2024; Accepted: August 29, 2024; Available online: August 29, 2024.

DOI: 10.46770/AS.2024.121

ABSTRACT: Advancements in Zn isotope analytical methods and their widespread application in geosciences underscore the importance of the purification process in isotopic measurements. Efficient purification of Zn, which involves separating Zn from matrix elements, is essential for accurately determining Zn isotopic compositions. This study proposes an optimized purification method that combines precipitation and a chromatographic procedure, significantly enhancing the purification efficiency. Using the established purification process, nine widely available geological-certified reference materials with known Zn isotopic compositions yield $\delta^{66}\text{Zn}$ values that are in agreement with most previously published data within two standard deviations (2s) of repeat measurements. In addition, the effects of the presence of matrix elements have been evaluated using Neptune Plus MC-ICP-MS in a wet plasma mode. The average $\delta^{66}\text{Zn}$ value of the multi-elemental Zn standard GSB-1, prepared by adopting GSB with different matrix elements, demonstrates good consistency with the long-term measured value of the pure GSB-Zn solution after precipitation and chromatographic separation. This enhanced purification protocol for Zn isotope measurement applies to a diverse range of geological samples and reduces the time and chemical reagents required for purification compared to conventional methods.

INTRODUCTION

Zinc, a moderately volatile transition metal, has the lowest atomic mass of the Group 12 elements. It has five stable isotopes of ^{64}Zn , ^{66}Zn , ^{67}Zn , ^{68}Zn , and ^{70}Zn , with relative abundances of 48.63%, 27.90%, 4.10%, 18.75% and 0.62%, respectively.¹ Zn predominantly exists in its metallic form Zn^0 or as the oxidation state Zn^{2+} , found mainly in aerosols, the hydrosphere, biosphere, and silicate Earth. Zn is dominantly lithophile and slightly siderophile depending on environmental conditions.² The stable isotope compositions of Zn provide critical insights into Earth sciences, enhancing understanding in areas of ore formation, oceanography, geochemical weathering, early solar system processes, and mantle geochemistry.³

Zn isotopic analysis has revealed significant isotopic

fractionation in natural biological and terrestrial geological samples, with variations in $\delta^{66}\text{Zn}$ of up to 2‰ (defined as ‰ deviation of $^{66}\text{Zn}/^{64}\text{Zn}$ ratio relative to the JMC-Lyon certified reference material) at or near the Earth's surface under low temperature and pressure conditions.^{3,4} In contrast, Zn isotopes in magmatic reservoirs exhibit less variation, commonly ranging from 0.1 to 0.3‰.⁵⁻⁷ To detect these small variations, highly precise and accurate isotopic measurements are required. Zinc isotope ratios were first measured using thermal ionization mass spectrometry (TIMS) in the 1950s with analytical errors of 0.1‰ or greater,⁸ which hindered the applications of Zn isotopes to geological processes. Over the past few decades, a wealth of Zn isotope data have been determined using multi-collector inductively coupled plasma-mass spectrometry (MC-ICP-MS) following the pioneering Zn isotope study by Maréchal *et al.* (1999).⁹ To limit the mass discrimination effect and time drift

effects during mass spectrometry measurements, different correction schemes have been employed, such as "standard-sample bracketing" (SSB),^{5,10,11} elemental doping (Cu correction)¹²⁻¹⁵ or double spike.¹⁶⁻²⁰

Zn stable isotope measurement is typically performed using multi-collector inductively coupled plasma-mass spectrometry (MC-ICP-MS), where samples are introduced into the mass spectrometer in a dilute acid solution using a concentric nebulizer and spray chamber sample introduction system. Most research groups using this method report an analytical precision of ~0.05% (2s of replicate analyses) and evaluate their precision and accuracy by analyzing pure Zn solution standards as well as natural reference materials (RMs). However, Zn isotope MC-ICP-MS analysis is sensitive to isobaric interferences and non-isobaric matrix effects, necessitating chemical purification of Zn and its separation from sample matrices prior to analysis. Maréchal *et al.* (1999)⁹ established a procedure, now widely used, to separate Zn from geological samples using anion exchange resin. Since this publication, separation techniques have been refined by many studies aiming to improve the purity of the separated Zn fractions, reduce the acid volumes needed, and consequently minimize the analytical blank contributions from ion exchange procedures.^{12, 14, 21-23} Sossi *et al.* (2015)¹⁴ developed an optimized separation methodology using AG1-X8 resin to separate Cu, Fe, and Zn from each other and matrix elements in diverse rock samples. Their optimized method has minimized the preparation time, reagent consumption and total analytical blanks.

The multi-column ion exchange method involves purifying elements by sequentially using ion exchange resins multiple times. After an initial ion exchange resin separation, the eluate is collected and evaporated to change the medium, then subjected to another ion exchange to further purify the target element. Multi-column ion exchange chromatography is an efficient separation technique widely applied in high-precision analysis of Zn isotopes. This method is particularly well-suited for geological samples, including rocks, soils, sediments, and aqueous samples, among others, due to its ability to provide high-purity Zn isotope separation and achieve a Zn recovery rate close to 100%. Zhai *et al.* (2023)²⁴ have developed a two-step Zn chemical separation protocol utilizing Bio-Rad AG MP-1M resin columns. This method has demonstrated excellent reproducibility for measuring the external $\delta^{66}\text{Zn}$ values (relative to JMC-Lyon) of standard soil reference materials over an extended time period, with a better than 0.06‰ (2SD) precision. While this method generally offers high separation efficiency for the target element from matrix elements, it heavily relies on ion exchange columns, resulting in cumbersome and lengthy procedures. Additionally, the substantial consumption of inorganic acid reagents makes it impractical for large-scale sample separations.

Precipitation, a common method for separation and enrichment

of trace elements,²⁵ effectively isolates target elements from matrix elements. Metal hydroxide co-precipitation, in particular, is highly efficient, allowing for rapid separation of precipitate from supernatant through centrifugation. This process, featured with a high recovery rate, is often used for the separation and enrichment of trace and ultra-trace elements in rock and water samples. To further improve isotope separation efficiency, some scholars have used precipitation pre-enrichment for isotope separation and enrichment. For example, Bao *et al.* (2019)²⁶ utilized precipitation followed by dual ion exchange resin methods for separation and purification, accurately determining Mg isotope ratios. Liu *et al.* (2020)²⁷ combined precipitation with a single ion exchange resin method to separate and purify Sr elements from high Rb/Sr samples, accurately determining their isotope ratios. These advancements highlight the significance of precipitation in element separation and purification in geological research.

To separate a purer zinc solution from geological rock samples with complex matrices, traditional methods typically employ a two-step ion exchange chromatography before analysis via the MC-ICP-MS. In this study, we innovated by combining a precipitation step with chromatographic processing to purify the sample solution, allowing the processing of more samples in a short time frame and with reduced eluent consumption. Our findings demonstrate that this purification process is more efficient than conventional two-step ion exchange chromatography purification methods for geological samples.^{23, 28}

The matrix effects of ten elements (Na, Mg, Al, K, Ti, Cr, Mn, Fe, Ni and Cd) were also evaluated. During the solution nebulization multi-collector inductively coupled plasma mass spectrometry (SN-MC-ICP-MS) analyses, the instrumental mass bias was corrected using the SSB technique, with Cu as an internal standard. Our results demonstrate that our refined efficient Zn purification process enables precise determination of Zn isotopes, and the Zn isotopic compositions of nine different types of reference materials measured are consistent with established data. The accurate determination of the Zn isotopes in these reference materials attests to the suitability of this novel purification procedure for analysis of various rocks.

EXPERIMENTAL

Reagents and reference materials. Sample digestion and purification were performed under Class 100 laminar flow hoods in a Class 1000 cleanroom at the State Key Laboratory of Continental Dynamics (SKLCD) to reduce the process blank of Zn and avoid cross-contamination. Ultrapure water (MQ-H₂O) with a resistivity of 18.2 M Ω cm⁻¹ was obtained from a Milli-Q Element water purification system (Millipore, Billerica, MA, USA). Commercially available hydrofluoric acid (HF, 40% (v/v), GR grade), nitric acid (HNO₃, 68% (v/v), GR grade), and

Table 1. Details of the Zn separation procedure using precipitation and chromatographic exchange resin AG1-X8

	Reagent/reaction	Amount/time	Comments
Stage 1 (repeat twice)	30% NH ₄ OH	Adjust the pH ≈ 12	Precipitation
	Ultrasonic	15 min	
	Centrifugation	5000 rpm for 10 min	Collect the supernatant
Stage 2 (AG1-X8 resin)	3 mol L ⁻¹ HNO ₃	10 mL	Resin cleaning
	Milli-Q H ₂ O	10 mL	Resin cleaning
	6 mol L ⁻¹ HCl	10 mL	Resin cleaning and conditioning
	6 mol L ⁻¹ HCl	1 mL	Sample loading
	6 mol L ⁻¹ HCl	5 mL	Removal of most matrix elements
	6 mol L ⁻¹ HCl	14 mL	Removal of Cu and Co
	0.5 mol L ⁻¹ HCl	9 mL	Removal of Fe, Ga and Mo
	3 mol L ⁻¹ HNO ₃	5 mL	Zn collection

hydrochloric acid (HCl, 36% (v/v), GR grade) were purified twice using a sub-boiling distillation system via Savillex DS-1000 (Minnetonka, MN, USA). 1 mL of Bio-Rad AG1-X8 (200–400 mesh, USA) anion exchange resin was loaded into a Bio-Rad Poly-Prep column with a diameter of 8 mm and a length of 9 cm. All beakers, Teflon bottles, and PFA vials were respectively cleaned with GR grade HNO₃, high-pure HNO₃, and deionized water for 24 h on a hot plate (120 °C) in sequence. All acids and mixed acids used for column elution were prepared according to molar concentration and volume, and their strength was precisely determined by titration with sodium hydroxide titration solution. Ammonium hydroxide aqueous solution was purchased from Sinopharm Chemical Reagent (China).

Two pure Zn solutions, NIST SRM 683 and NIST SRM 682 were used as in-house Zn standards in the SKLCD. NIST SRM 683, produced by the National Institute of Standards and Technology (NIST), is certified to be a good international reference material for Zn isotope measurement, and its $\delta^{66}\text{Zn}_{\text{JMC-Lyon}}$ value is $0.12 \pm 0.04\%$ relative to the certified reference material (CRM) JMC-Lyon.²⁹ NIST SRM 682, with the $\delta^{66}\text{Zn}_{\text{JMC-Lyon}}$ value of $-2.45\% \pm 0.02\%$,³⁰ was used as an unknown sample for quality control. A pure concentrated single-element solution Zn (GSB 62025-90, 1000 $\mu\text{g mL}^{-1}$ in 10% HCl) was purchased from Guobiao (Beijing) Testing & Certification Company (China). GSB-1 is a multi-element solution consisting of matrix elements (Na: Mg: Al: K: Ca: Fe: Cu: Zn = 100: 100: 100: 100: 100: 100: 1: 1), and it was used to validate the Zn purification procedures. The matrix effects of Na, Mg, Al, K, Ti, Cr, Mn, Fe, Ni and Cd on Zn were investigated by adding various amounts of each element to NIST SRM 683.

The samples analyzed in this study include GSP-2 (granodiorite, USGS), AGV-2 (andesite, USGS), W-2 (diabase, USGS), BCR-2 (basalt, USGS), BHVO-2 (basalt, USGS), NOD-A-1 (manganese nodule, USGS), GBW07103 (GSR-1, granite, CNRCG), GBW07104 (GSR-2, andesite, CNRCG), and GBW07105 (GSR-3, basalt, CNRCG). These reference materials with certified Zn isotopes were selected to evaluate the stability of the innovative method.

Sample preparation and Zn purification. Depending on the Zn mass fraction of samples, whole rock powders (of 10–150 mg) containing about 4 μg of Zn were dissolved using concentrated HNO₃ and HF (2:1 volume ratio) acid in 15 mL pre-cleaned PFA vials on the hot plate at 120 °C for 2 days. Following the evaporation of HNO₃ and HF, the dried samples were refluxed with concentrated HNO₃ on the hot plate at 80 °C for 1 day to remove residual fluoride and dried again before being digested with a 1:3 volume mixture of concentrated HNO₃ and HCl to ensure complete dissolution. The dried residue was refluxed with concentrated HNO₃, then the digest solutions were dried twice in 0.5 mL of concentrated HNO₃. Finally, sample solutions were taken up in 1 mL diluted HNO₃ and transferred to a 15 mL centrifuge tube. Then, ammonium hydroxide aqueous solution was added to the sample solution, adjusting the solution pH to approximately 12. This process precipitated nearly all the Fe, Mg, and V as hydroxides, while Zn was dissolved in the form of a complex ion in the excess ammonia water. Additionally, the 15 minutes' ultrasonic bath contributed to precipitation. This is a critical step in our experiment as it effectively separates the desired element. To extract Zn from the solution, the solution was centrifuged at 5000 rpm for 10 minutes, and the supernatant was collected. The precipitation process was repeated twice to prevent isotopic fractionation of Zn. The column chromatography was conducted at the SKLCD, following the procedure described by Sossi *et al.* (2015).¹⁴ Following precipitation, a one-column Zn chromatographic procedure was carried out using Bio-Rad columns charged with 1 mL Bio-Rad AG1-X8 200–400 mesh (0.038–0.075 mm resin bead diameter) anion exchange resin. The resin is a strongly basic anion exchange resin, which comprises polymerized styrene cross-linked by divinylbenzene. Prior to the chromatographic procedure, the resin was backwashed using a pipette to eliminate any air bubbles. The resin was sequentially cleaned by flowing 3 mol L⁻¹ HNO₃, Milli-Q water, and 6 mol L⁻¹ HCl through the columns (Table 1), where the final step cleans matrix elements and conditions the resin by converting it into chloride form.¹⁴ All samples were evaporated to dryness, then all dried samples were redissolved with 1 mL of 6 mol L⁻¹ HCl and loaded onto the columns, followed by loading 5 mL of 6 mol L⁻¹ HCl to elute most matrix elements (e.g., K, Ca, Na, Mg, Al, Ni, Ti,

Fig. 1 Elution curves obtained during Zn purification procedures of GSR-3 rock standard in 1 mL AG1-X8 (200 – 400 mesh).

Table 2. Instrumental operating parameters for Zn isotope measurements

Instrumental parameters	Neptune Plus MC-ICP-MS
Coolant gas	15 L min ⁻¹ Ar
Auxiliary gas	0.8 L min ⁻¹ Ar
Nebulizer gas	1.05 L min ⁻¹ Ar
RF power	1200 W
Accelerate voltage	10 000 V
Sampling cone	Ni, standard cone
Skimmer cone	Ni, H cone
Nebulizer	PFA 50 μL min ⁻¹
Resolution mode	Medium
Integration time	40 cycles with 4.194 s per cycle

Mn, Ba, Sr, and so on). The Cu and Co were eluted in the next 14 mL of 6 mol L⁻¹ HCl, followed by 9 mL of 0.5 mol L⁻¹ HCl for Fe, Ga, and Mo. The Zn fraction was collected with 5 mL of 3 mol L⁻¹ HNO₃, which was evaporated to dryness and dissolved twice in concentrated HNO₃ to remove all chlorine (Fig. 1). Finally, all sample solutions were diluted to 1 μg g⁻¹ with 2% HNO₃ (v/v) for isotopic measurements.

To validate the Zn chromatographic procedure described above, every 1 mL of eluate was continuously collected for the determination of major and trace element concentrations using Agilent 8900 at the SKLCD. All columns employed for the Zn chromatographic procedure were calibrated using an alkali-olivine basalt reference material (GSR-3). The detailed Zn separation procedure combining the precipitation and ion chromatography processes can be found in Table 1 and Fig. 1.

Mass Spectrometry. Zinc isotopic measurements were determined using a double-focusing MC-ICP-MS (Neptune Plus, Thermo Fisher Scientific, Bremen, Germany) at the SKLCD. This instrument is equipped with eleven Faraday cups and five discrete dynode multipliers. In static mode, L3, L2, L1, C, H1, H2 and H3 Faraday cups fitted with 10¹¹Ω amplifier resistors were used to

collect ⁶²Ni, ⁶³Cu, ⁶⁴Zn, ⁶⁵Cu, ⁶⁶Zn, ⁶⁷Zn and ⁶⁸Zn, respectively, where the ⁶²Ni monitor corrected the interference of ⁶⁴Ni on ⁶⁴Zn. The sample solutions were introduced using an autosampler (ASX-112FR; Cetac Technologies, Omaha, NE, USA). Zn isotope ratios were measured in a wet plasma mode (Table 2) with a standard sampler cone, H skimmer cone, and a cyclone/double-pass quartz spray chamber with a PFA concentric nebulizer at a low flow rate of 50 mL min⁻¹ (SIS, Stable Introduction System). The instrumental mass bias was corrected by the SSB method combined with NWU-Cu-B Cu as an internal reference material. NWU-Cu-B Cu exhibits a ⁶⁵Cu/⁶³Cu ratio of 0.44689 as determined by MC-ICP-MS.³¹ The in-house standard solution, NIST SRM 683 provided by Chen *et al.* (2016),¹⁵ was used as the reference standard for Zn isotope measurement. Zinc isotope ratios were measured in a medium-resolution mode to resolve polyatomic interferences, such as ⁴⁸Ti¹⁶O⁺, ²⁸Si³⁶Ar⁺, and ⁴⁸Ca¹⁶O⁺ for ⁶⁴Zn⁺, ⁵⁰Ti¹⁶O⁺, ⁵⁰Cr¹⁶O⁺, ⁴⁸Ti¹⁸O⁺, and ¹³²Ba²⁺ for ⁶⁶Zn⁺, ⁵¹V¹⁶O⁺, ²⁷Al⁴⁰Ar⁺ and ¹³⁴Ba²⁺ for ⁶⁷Zn⁺, and ²⁸Si⁴⁰Ar⁺, ³²S³⁶Ar⁺ and ¹³⁶Ba²⁺ for ⁶⁸Zn⁺. Zinc isotope ratios were expressed as a per mil deviation relative to the reference material NIST SRM 683 and then converted into values relative to the reference material JMC-Lyon Zn:

$$\delta^{66}\text{Zn}_{\text{JMC-Lyon}} = [(\frac{^{66}\text{Zn}}{^{64}\text{Zn}})_{\text{sample}} / (\frac{^{66}\text{Zn}}{^{64}\text{Zn}})_{\text{NIST SRM 683}} - 1] \times 1000] + 0.12 \quad (1)$$

$$\delta^{67}\text{Zn}_{\text{JMC-Lyon}} = [(\frac{^{67}\text{Zn}}{^{64}\text{Zn}})_{\text{sample}} / (\frac{^{67}\text{Zn}}{^{64}\text{Zn}})_{\text{NIST SRM 683}} - 1] \times 1000] + 0.18 \quad (2)$$

$$\delta^{68}\text{Zn}_{\text{JMC-Lyon}} = [(\frac{^{68}\text{Zn}}{^{64}\text{Zn}})_{\text{sample}} / (\frac{^{68}\text{Zn}}{^{64}\text{Zn}})_{\text{NIST SRM 683}} - 1] \times 1000] + 0.24 \quad (3)$$

RESULTS AND DISCUSSION

Purification of Zn. During the sample digestion, precipitation, and chromatographic processes, attributed to the utilization of high-purity chemical reagents and rigorously cleaned beakers and columns, the total procedural blank for Zn remained below 32 ng, of which approximately 24 ng is contributed by ammonium hydroxide. The ratio of the procedural Zn blank to the Zn loaded onto the column was less than 0.008, indicating that the Zn present in the procedural blank was negligible in comparison to the 4 μg of Zn processed. ICP-MS analysis of the Zn blank confirmed that the procedural blanks for all elements in the matrix were within acceptable limits. Measurements of Zn isotopes indicated that the blank intensities of ⁶⁴Zn were typically below 5 mV in a 2% HNO₃ solution. Zn recovery from geological standards was 98.3% following precipitation with ammonia water and 98.6% after chromatographic purification. The minor loss of supernatant may be attributed to the incomplete separation between the supernatant and the precipitate, but it does not induce fractionation of Zn isotopes.

Fig. 2 Variations in the measured $\delta^{66}\text{Zn}$ values of NIST SRM 683 standard solutions spiked with different amounts of Na, Mg, Al, K, Ti, Cr, Mn, Fe, Ni, and Cd. The x-axis represents the element mass fraction in the solution relative to that of Zn ($1 \mu\text{g g}^{-1}$ for all samples). The errors were obtained from four replicate measurements. The grey horizontal area represents the 2s range of $\pm 0.05 \text{ ‰}$.

The precipitation process efficiently removed approximately 99.9% Fe, 99.7% Ba, 99.7% V, 99.2% Ca, 96.3% Mg, and 96.7% Ti from the sample, with no significant Zn isotopic fractionation observed. To verify the purification process, the concentrations of matrix elements in the eluted solution were also determined using ICP-MS. The concentrations of these matrix elements were substantially lower than that of Zn, resulting in a ratio of Zn to the sum of major elements $(\text{Na} + \text{Mg} + \text{Al} + \text{K} + \text{Ca} + \text{Fe})/\text{Zn} < 0.05$. The individual ratios were as follows: $\text{Na}/\text{Zn} < 0.015$, $\text{Mg}/\text{Zn} < 0.002$, $\text{Al}/\text{Zn} < 0.003$, $\text{K}/\text{Zn} < 0.002$, $\text{Ca}/\text{Zn} < 0.015$, $\text{Fe}/\text{Zn} < 0.015$, $\text{Mn}/\text{Zn} < 0.0001$, $\text{Cu}/\text{Zn} < 0.0005$, $\text{Cd}/\text{Zn} < 0.0005$, $\text{Cr}/\text{Zn} < 0.00005$, $\text{Ti}/\text{Zn} < 0.0005$, and $\text{Ni}/\text{Zn} < 0.0001$. Additionally, a comparison of the residual matrix elements for the natural

reference material GSR-3 was conducted both with and without the precipitation step, following purification through chromatographic procedures. A notable difference was observed in the ratio of Fe to Zn in the residual matrix elements, which was 0.35 after chromatographic separation without precipitation. However, after both precipitation and chromatographic separation, this ratio decreased to 0.01. Thus, the developed purification procedure effectively removed matrix elements, thereby minimizing the matrix effect during instrumental analysis.

Matrix effect. When conducting zinc isotope analysis via MC-ICP-MS, effective removal of matrix elements by chemical purification is essential for collecting Zn solution. Despite the removal of the majority of matrix elements during the established purification procedure, residual trace elements in the purified solution may still affect the determination of isotope ratios, as the ratio of each matrix element to Zn varies. These trace elements can cause signal interference in the mass spectrometer, affecting the precision and accuracy of Zn isotopic determination. In this case, it can no longer be assumed that the instrumental mass bias of the pure Zn standard can represent that of the bracketed sample. In this study, the effects of Na, Mg, Al, K, Ti, Cr, Mn, Fe, Ni and Cd on the accuracy of Zn isotopic measurements were investigated by using Neptune Plus MC-ICP-MS in a wet plasma mode. The impact of matrix elements on Zn isotope analysis was investigated by comparing a series of solutions of $1 \mu\text{g g}^{-1}$ NIST SRM 683 Zn and 500 ng g^{-1} NWU-Cu-B Cu, each doped with varying proportions of a single matrix element (with matrix/Zn ratios ranging from 0.001 to 10). These were bracketed against the pure solution of $1 \mu\text{g g}^{-1}$ NIST SRM 683 Zn and 500 ng g^{-1} NWU-Cu-B Cu. Among these matrix elements, some are primary constituents of geological samples, while others are difficult to separate completely from Zn using anion exchange resin, serving as ideal candidates for doping experiments to evaluate the precision of our method.

Figure 2 shows the correlation between $\delta^{66}\text{Zn}$ values and the mass fraction ratios of matrix elements to Zn. The analysis reveals that the accuracy of Zn isotope measurements varies with different matrix constituents. Notably, the $\delta^{66}\text{Zn}$ measurement is affected by the presence of Ni and Ti, due to significant isobaric interferences of $^{64}\text{Ni}^+$ and $^{48}\text{Ti}^{16}\text{O}^+$ on $^{64}\text{Zn}^+$.³² And therein, when $C_{\text{Ti}}/C_{\text{Zn}} > 0.01$ and $C_{\text{Ni}}/C_{\text{Zn}} > 0.2$, significant offsets in $\delta^{66}\text{Zn}$ and $\delta^{67}\text{Zn}$ are observed. Although $\delta^{66}\text{Zn}$ and $\delta^{67}\text{Zn}$ values are less sensitive to other elements compared to Ni and Ti, the addition of common matrix elements Na, K, Mg and Al in silicate rocks still significantly affects the precision and accuracy of Zn isotope determination. For instance, with the presence of Na and K, $C_{\text{Na}}/C_{\text{Zn}} > 1$ and $C_{\text{K}}/C_{\text{Zn}} > 3$ generally skew apparent Zn isotope compositions towards heavier values. When $C_{\text{Mg}}/C_{\text{Zn}}$ exceeds 1, $\delta^{66}\text{Zn}$ shifts towards lighter values and $\delta^{67}\text{Zn}$ towards heavier values. When $C_{\text{Al}}/C_{\text{Zn}} > 1$, $\delta^{67}\text{Zn}$ is significantly shifted towards heavier values, though $\delta^{66}\text{Zn}$ remains unaffected up to $C_{\text{Al}}/C_{\text{Zn}} \leq 10$.

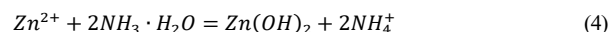
Fig. 3 Influence of varying additions of internal standard Cu on Zn isotopic measurements.

of Zn isotopic ratio measurements, we conducted a series of experiments to determine the optimal additive quantity of copper as an internal standard at various Cu/Zn molar ratios, thereby avoiding matrix interference. Our experimental design involved the use of mixed solutions containing pure zinc solution NIST SRM 683 and pure copper solution NWU-Cu-B, spanning a range of Cu/Zn molar ratios from 0.05 to 10, simulating the quantities of internal standard that might be added in practical isotopic analyses.

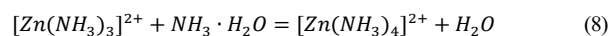
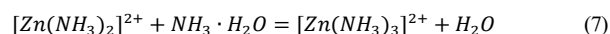
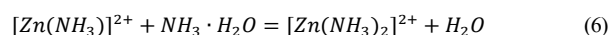
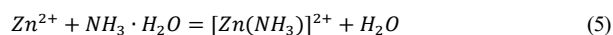
As illustrated in Fig. 3, the results indicate a remarkable consistency in the measured Zn isotopic ratios across the Cu/Zn molar ratios spanning from 0.05 to 10, with results falling well within the error margins, thereby validating the accuracy of our methodology. These data indicate that the amount of copper added as an internal standard, relative to zinc within the range of 0.05 to 10, can effectively correct for mass bias. Our results demonstrate the robustness of Cu as an internal standard for Zn isotope analysis across a wide range of Cu/Zn molar ratios.

The effect of different pH conditions during precipitation.

While adding ammonium hydroxide to the geological sample solution, its pH value gradually increases from the rising alkalinity of the solution, leading to a reaction between zinc ions and ammonium hydroxide to form zinc hydroxide.



Zinc hydroxide is an amphoteric hydroxide that is slightly soluble in water. As the concentration of ammonium hydroxide in the solution increases, zinc hydroxide undergoes a gradual hydrolysis reaction with ammonium hydroxide.



Adding an excess of ammonia water to a geological sample solution causes zinc ions to form the $[\text{Zn}(\text{NH}_3)_4]^{2+}$ complex ion through a complexation reaction with ammonia. This complexation is pH-dependent, with greater stability at higher pH levels, thus increasing the solubility of zinc. The complexation process is primarily determined by stoichiometric factors and pH, with the presence of other species, such as iron hydroxide, which is a chemical compound that can form under certain conditions, exerting a negligible influence on the reaction kinetics. Therefore, the presence of iron hydroxide does not alter the fundamental workings of the process being discussed. Eventually, zinc exists in the form of zinc-ammonia complex ions, which are present in the supernatant. This process depends on the pH value of the solution but is independent of the presence of iron hydroxide.

Fig. 4 Effect of pH during precipitation.

Less notable offset is found in $\delta^{66}\text{Zn}$ and $\delta^{67}\text{Zn}$ when $C_{\text{Fe}}/C_{\text{Zn}} \leq 0.5$, $C_{\text{Mn}}/C_{\text{Zn}} \leq 1$, $C_{\text{Cd}}/C_{\text{Zn}} \leq 5$ and $C_{\text{Cr}}/C_{\text{Zn}} \leq 1$, indicating minimal impact on both isotopes. The isotopic analysis of Zn can be affected by the presence of these elements that form polyatomic ions with similar mass-to-charge ratios as the Zn isotopes of interest. For example, Mg can form polyatomic ions with Ar, such as $^{24}\text{Mg}^{40}\text{Ar}^+$, and $^{26}\text{Mg}^{40}\text{Ar}^+$, which can interfere with the analysis of $^{64}\text{Zn}^+$ and $^{66}\text{Zn}^+$, respectively. Cr can form $^{50}\text{Cr}^{16}\text{O}^+$ and $^{52}\text{Cr}^{16}\text{O}^+$, which could interfere with $^{66}\text{Zn}^+$ and $^{68}\text{Zn}^+$. Al can form $^{27}\text{Al}^{40}\text{Ar}^+$, which interferes with $^{67}\text{Zn}^+$. Ba can form doubly charged ions such as $^{132}\text{Ba}^{2+}$ and $^{134}\text{Ba}^{2+}$, which could interfere with $^{66}\text{Zn}^+$ and $^{67}\text{Zn}^+$, respectively. Ni and Ti can form $^{64}\text{Ni}^+$ and $^{48}\text{Ti}^{16}\text{O}^+$, which interfere with $^{64}\text{Zn}^+$. Additionally, $^{50}\text{Ti}^{16}\text{O}^+$ and $^{48}\text{Ti}^{18}\text{O}^+$ can interfere with $^{66}\text{Zn}^+$. Compared with Ni and Ti, $\delta^{66}\text{Zn}$ and $\delta^{67}\text{Zn}$ are less sensitive to the presence of most matrix elements, but the presence of high concentrations of Na, K, Mg, Al, Fe, Mn, Cd and Cr may still cause matrix effects, thereby reducing the precision and accuracy of Zn isotope determination.

Copper serves as a dopant employed to correct for fluctuations in mass bias during Zn isotopic analysis. To ensure the accuracy

Fig. 5 (a) Long-term measurements of mono-element standard solution yielded $\delta^{66}\text{Zn}_{\text{JMC-Lyon}} = -2.41 \pm 0.03\text{‰}$ (2s, n = 34) for NIST SRM 682; (b) Long-term measurements of mono-element standard solution yielded $\delta^{66}\text{Zn}_{\text{JMC-Lyon}} = 0.11 \pm 0.03\text{‰}$ (2s, n = 20) for GSB-Zn. The errors were obtained from three or four replicate measurements and the grey horizontal areas represent the 2s range of $\pm 0.03\text{‰}$.

Fig. 6 Long-term reproducibility of the $\delta^{66}\text{Zn}$ measurements of the purified multi-element synthetic solutions GSB-1. Errors were obtained by repeating the measurement four times. The grey horizontal area represents the 2s range of $\pm 0.02\text{‰}$.

In the precipitation process, pH conditions significantly influence the behavior of elements. As mentioned above, zinc exhibits a pattern of initial precipitation followed by subsequent release during pH fluctuations. By adjusting the pH conditions within an appropriate range, the separation of zinc from certain matrix elements can be achieved.

To investigate the effect of varying pH conditions on isotopic ratios post-chromatography during the precipitation process, we gradually added ammonium hydroxide aqueous solution to the multi-element synthetic solution GSB-1 using a micropipette. The pH adjustments were continuously monitored with a pH meter,

establishing a pH gradient (pH = 10.5, 11, 11.5, 12, 12.5). After the chromatography, Zn isotopic ratios were measured using MC-ICP-MS, and the optimal pH range for precipitation was determined based on the experimental results (Fig. 4). The results reveal that significant fractionation of Zn isotopes occurs at pH < 11.5, leading to large deviations from the long-term measured value of the pure GSB-Zn solution. With the increase in pH value, the fractionation of Zn isotope decreases. When the pH ≥ 11.5 , the Zn isotopic ratios align with the reference value of GSB-Zn within the 2s uncertainty intervals. By adjusting the pH, complete recovery of Zn from the sample solution into the supernatant is achievable, with the ideal pH for this precipitation process around 12.

Precision and accuracy. The precision and accuracy of our newly established method have been assessed by conducting replicated measurements of pure Zn solutions (NIST SRM 682 and GSB-Zn), the multi-element synthetic solutions GSB-1, and certified reference materials with published Zn isotopic compositions. Nine geological reference materials underwent at least three independent digestions each. The purification of the GSB-1 was repeated 8 times. Repeated measurements of these Zn solutions were performed using MC-ICP-MS in this study.

During this study, the long-term precision of Zn isotopic measurements was evaluated by repeated analyses of mono-element solutions of NIST SRM 682 and GSB-Zn over 6 months. The mean value of $\delta^{66}\text{Zn}_{\text{JMC-Lyon}}$ for NIST SRM 682 is $-2.41 \pm 0.03\text{‰}$ (2s, n = 34) (Fig. 5a), identical to the value reported by Nie *et al.* (2021)³³ in 2s. We also obtained that the average value of $\delta^{66}\text{Zn}_{\text{JMC-Lyon}}$ of GSB-Zn is $0.11 \pm 0.03\text{‰}$ (2s, n = 20) (Fig. 5b). The long-term precision of 0.03‰ (2s) demonstrates the stability of the instrument prior to analyzing standard solutions.

Table 3. Zinc isotope ratios of geological certified reference materials

Sample	Type	Zn ($\mu\text{g g}^{-1}$)	References	$\delta^{66}\text{Zn}$	2s	$\delta^{67}\text{Zn}$	2s	$\delta^{68}\text{Zn}$	2s	n				
BCR-2	Basalt	125	This study	0.26	0.02	0.39	0.05	0.52	0.05	10				
			Wang <i>et al.</i> (2017) ⁵	0.27	0.03									
			Li <i>et al.</i> (2019) ¹⁰	0.26	0.02									
			Chen <i>et al.</i> (2016) ¹⁵	0.25	0.04									
BHVO-2	Basalt	99	This study	0.33	0.03	0.52	0.06	0.68	0.06	15				
			Wang <i>et al.</i> (2023) ²⁸	0.32	0.03						0.49	0.04	0.64	0.03
			Wang <i>et al.</i> (2017) ⁵	0.31	0.04									
			Doucet <i>et al.</i> (2016) ³⁹	0.35	0.02									
			Rosca <i>et al.</i> (2021) ²⁰	0.36	0.03									
GSR-3	Basalt	150	This study	0.43	0.04	0.67	0.05	0.87	0.06	5				
			Wang <i>et al.</i> (2023) ²⁸	0.43	0.02						0.66	0.04	0.85	0.05
			Han <i>et al.</i> (2024) ³⁴	0.44	0.02									
			Lv <i>et al.</i> (2016) ³⁵	0.44	0.05									
AGV-2	Andesite	81	This study	0.30	0.03	0.45	0.08	0.59	0.07	10				
			Chen <i>et al.</i> (2016) ¹⁵	0.28	0.05									
			Wang <i>et al.</i> (2020) ³⁶	0.30	0.03									
			Amet and Fitoussi (2020) ¹⁸	0.34	0.02									
GSR-2	Andesite	50	This study	0.27	0.01	0.41	0.04	0.55	0.02	4				
GSP-2	Granodiorite	80	This study	1.01	0.09	1.40	0.12	1.65	0.15	9				
			Chen <i>et al.</i> (2016) ¹⁵	1.07	0.06									
			Doucet <i>et al.</i> (2018) ³⁹	1.08	0.02									
			Doucet <i>et al.</i> (2018) ³⁹	1.03	0.04									
GSR-1	Granite	29	This study	0.39	0.03	0.57	0.05	0.76	0.06	7				
			Han <i>et al.</i> (2024) ³⁴	0.40	0.04									
W-2	Diabase	80	This study	0.23	0.02	0.36	0.04	0.46	0.05	11				
			Chen <i>et al.</i> (2016) ¹⁵	0.22	0.05									
			Huang <i>et al.</i> (2018) ³⁷	0.23	0.05									
NOD-A-1	Manganese nodule	587	This study	0.98	0.01	1.48	0.03	1.96	0.02	3				
			Chen <i>et al.</i> (2016) ¹⁵	0.96	0.03									

Note: Zn isotopes are relative to JMC-Lyon; n represents the number of independent digests of each geological reference material and each purified sample solution was measured 3 or 4 times by MC-ICP-MS; 2s = 2 standard deviations of n repeat measurements.

The precision of $\delta^{66}\text{Zn}_{\text{JMC-Lyon}}$ determined by repeated analyses of these geological reference materials with independent digestions ranges from 0.01‰ to 0.09‰ (2s) with an average value of 0.03‰. The $\delta^{66}\text{Zn}_{\text{JMC-Lyon}}$ values obtained for these geological certified reference materials using the Neptune Plus MC-ICP-MS are in good agreement with the literature data (Table 3).

The accuracy of our method was further verified through determination of the synthetic standard made of GSB-1 with multiple matrix elements. Following the precipitation, chromatographic procedure and analytical methods described previously, the average Zn isotopic composition obtained was $\delta^{66}\text{Zn}_{\text{JMC-Lyon}} = 0.11 \pm 0.02\text{‰}$ (2s, n=8) (Fig. 6), indistinguishable from the pure GSB-Zn solution. Thus, the precipitation, the chromatographic procedure, and the MC-ICP-MS measurements developed in this study are robust and reproducible, with good accuracy and precision.

Zn isotope ratio of geological certified reference materials. To further validate the reliability of our newly developed purification method, we conducted experiments on a series of geological reference samples representing various rock types. Each sample underwent at least three independent digestions and was measured

more than three times using the MC-ICP-MS. The selected nine geological reference materials have Zn contents ranging from 29 to 587 $\mu\text{g g}^{-1}$, including basalts (BCR-2, BHVO-2 and GSR-3), andesite (AGV-2 and GSR-2), granodiorite (GSP-2), granite (GSR-1), diabase (W-2), and manganese nodule (NOD-A-1). The measured $\delta^{66}\text{Zn}_{\text{JMC-Lyon}}$ values of these geological reference materials obtained in this study and from previous studies are summarized in Table 3 and Fig. 7.

The mean $\delta^{66}\text{Zn}_{\text{JMC-Lyon}}$ values of basalts BCR-2 and BHVO-2 were $0.26 \pm 0.02\text{‰}$ (2s, n = 10) and $0.33 \pm 0.03\text{‰}$ (2s, n = 15), respectively. The $\delta^{66}\text{Zn}_{\text{JMC-Lyon}}$ values of BCR-2 and BHVO-2 were both consistent with the previously published data (Table 3). Our obtained average $\delta^{66}\text{Zn}_{\text{JMC-Lyon}}$ of GSR-3 was $0.43 \pm 0.04\text{‰}$ (2s, n = 5), agreeing well with the published values of $0.44 \pm 0.02\text{‰}$ (2s) by Han *et al.* (2024)³⁴ and $0.44 \pm 0.05\text{‰}$ (2s) by Lv *et al.* (2016)³⁵. The $\delta^{66}\text{Zn}_{\text{JMC-Lyon}}$ value of andesite AGV-2 was $0.30 \pm 0.03\text{‰}$ (2s, n = 10), consistent with the $0.28 \pm 0.05\text{‰}$ (2s) reported by Chen *et al.* (2016)¹⁵ and $0.30 \pm 0.03\text{‰}$ (2s) by Wang *et al.* (2020)³⁶. The average $\delta^{66}\text{Zn}_{\text{JMC-Lyon}}$ value of $0.27 \pm 0.01\text{‰}$ (2s, n = 4) in GSR-2 is in good agreement with that reported by Han *et al.* (2024)³⁴. The $\delta^{66}\text{Zn}_{\text{JMC-Lyon}}$ value of $1.01 \pm 0.09\text{‰}$ (2s, n = 9) for GSP-2 is slightly lower than that of $1.07 \pm 0.06\text{‰}$ (2s) reported

Fig. 7 $\delta^{66}\text{Zn}_{\text{JMC-Lyon}}$ values of nine geological reference materials, and comparison with the literature data. The blue symbols represent values obtained from different digestions in this study, while the red symbols represent values from the literature. Error bars represent two standard deviations (2s) of all replicates.

Fig. 8 (a) $\delta^{66}\text{Zn}_{\text{JMC-Lyon}}$ values of nine reference materials obtained in this study vs. reported values; (b) Zn three-isotope plot ($\delta^{67}\text{Zn}$ vs. $\delta^{66}\text{Zn}$) of certified reference materials analyzed in this study, purified by the established method. The slope of the linear regression is 1.49 ± 0.01 , consistent with the slope values of kinetic (1.48) and equilibrium (1.49) fractionation within error.

by Chen *et al.* (2016)¹⁵. The Zn isotopic composition of $0.39 \pm 0.03\text{‰}$ (2s) obtained for granite GSR-1 measured in this study agreed with reported values by Han *et al.* (2024)³⁴ within the reported uncertainty. The mean $\delta^{66}\text{Zn}_{\text{JMC-Lyon}}$ values of diabase W-2 with multiple digestion was $0.23 \pm 0.02\text{‰}$ (2s, $n = 11$), in agreement with that reported by Chen *et al.* (2016)¹⁵ and Huang *et al.* (2018)³⁷, respectively. NOD-A-1 has a $\delta^{66}\text{Zn}_{\text{JMC-Lyon}}$ value of $0.98 \pm 0.01\text{‰}$ (2s, $n = 3$), consistent with the $0.96 \pm 0.03\text{‰}$ (2s) reported by Chen *et al.* (2016)¹⁵. In summary, the Zn isotopes of all nine geological samples were accurately determined after purification (Fig. 8a). The consistency of the results verifies the accuracy and reliability of the improved method for isotopic analysis in different types of rocks.

The Zn three-isotope plots of all certified reference materials are

shown in Fig. 8b. The $\delta^{66}\text{Zn}$ and $\delta^{67}\text{Zn}$ fractionation line ($y = (1.49 \pm 0.01)x + (0.01 \pm 0.01)$, $R^2 = 0.999$) has a slope consistent with the kinetic (1.48) and equilibrium (1.49) fractionation within the error,³⁸ and the Zn isotopes of all these certified reference materials show mass-dependent fractionation.

CONCLUSION

In this study, we developed an efficient purification method combining precipitation with a subsequent column chromatography step to effectively separate Zn from matrix elements in geological samples, significantly reducing the consumption of chemical reagents while ensuring effective separation. The Zn isotope ratios were measured using the SSB

method combined with Cu as an internal standard by MC-ICP-MS. The matrix effects on the accurate and precise analysis of Zn isotopes were evaluated systematically by using Neptune Plus MC-ICP-MS. The measurement of Zn isotopes was accurate and precise when $C_{Na}/C_{Zn} \leq 1$, $C_K/C_{Zn} \leq 3$, $C_{Mg}/C_{Zn} \leq 1$, $C_{Al}/C_{Zn} \leq 1$, $C_{Fe}/C_{Zn} \leq 0.5$, $C_{Mn}/C_{Zn} \leq 1$, $C_{Cd}/C_{Zn} \leq 5$, $C_{Cr}/C_{Zn} \leq 1$, $C_{Ti}/C_{Zn} \leq 0.01$ and $C_{Ni}/C_{Zn} \leq 0.2$. In addition, when Cu is used as the internal standard in Zn isotope analysis, spanning a range of Cu/Zn molar ratios from 0.05 to 10, it can effectively correct the mass bias. The $\delta^{66}Zn$ values of the purified multi-element synthetic solution GSB-1 closely matched that of the pure Zn solution GSB-Zn. The $\delta^{66}Zn$ values of nine geological reference materials, as determined by the improved purification method, agree with the values reported in the literature. The long-term instrumental stability was confirmed by repeated analysis of the in-house standard NIST SRM 682 and pure GSB-Zn solution, yielding $\delta^{66}Zn$ of $-2.41 \pm 0.03\text{‰}$ (2s, n = 34) and $0.11 \pm 0.03\text{‰}$ (2s, n = 20), respectively.

ASSOCIATED CONTENT

The supporting information (Original data) is available at www.at-spectrosc.com/as/home.

AUTHOR INFORMATION



Hong-Lin Yuan received his PhD in 2002 from the China University of Geosciences (Wuhan). He is a research professor of Geology, Northwest University. His major research interests are in situ micro-analyses using femtosecond & nanosecond laser ablation - quadruple & multiple collector ICP-MS and its application in geochemistry, isotope geochemistry, analytical geochemistry. He has been working as member of editorial board for *Atomic Spectroscopy*. He has won the Sun Xian-Shu Award, the New Century Excellent Talents Support Program of Ministry of Education, the Hou Defeng Mineral and Rock Geochemical Young Scientist Award, and the World Laboratory Wilhelm Simon Fellowships, etc. He has published 140 SCI papers and obtained 8 Chinese invention patents and 2 US patents.

Corresponding Author

* H. L. Yuan

Email address: yhlskld@126.com

Notes

The authors declare no competing financial interest.

ACKNOWLEDGMENTS

This work was financially supported by the National Natural Science Foundation of China (42130102, 42173033, 42203035, and 42073051) and the MOST Research Foundation from the State Key Laboratory of Continental Dynamics.

REFERENCES

1. K. J. R. Rosman, *Geochim. Cosmochim. Acta*, 1972, **36**, 801-819. [https://doi.org/10.1016/0016-7037\(72\)90089-0](https://doi.org/10.1016/0016-7037(72)90089-0)
2. J. Siebert, A. Corgne, and F. J. Ryerson, *Geochim. Cosmochim. Acta*, 2011, **75**, 1451-1489. <https://doi.org/10.1016/j.gca.2010.12.013>
3. F. Moynier, D. Vance, T. Fujii, and P. Savage, *Rev. Mineral. Geochem.*, 2017, **82**, 543-600. <https://doi.org/10.2138/rmg.2017.82.13>
4. C. N. Maréchal, E. Nicolas, C. Douchet, and F. Albarède, *Geochem. Geophys. Geosy.*, 2000, **1**, 1015. <https://doi.org/10.1029/1999GC000029>
5. Z.-Z. Wang, S.-A. Liu, J. Liu, J. Huang, Y. Xiao, Z.-Y. Chu, X.-M. Zhao, and L. Tang, *Geochim. Cosmochim. Acta*, 2017, **198**, 151-167. <https://doi.org/10.1016/j.gca.2016.11.014>
6. J. Huang, S. Chen, X.-C. Zhang, and F. Huang, *J. Geophys. Res.-sol Ea.*, 2018, **123**, 2706-2722. <https://doi.org/10.1002/2017JB015287>
7. S.-A. Liu and S.-G. Li, *Engineering*, 2019, **5**, 448-457. <https://doi.org/10.1016/j.eng.2019.03.007>
8. R. Blix, H. v. Ubisch, and F. E. Wickman, *Geochim. Cosmochim. Acta*, 1957, **11**, 162-164. [https://doi.org/10.1016/0016-7037\(57\)90078-9](https://doi.org/10.1016/0016-7037(57)90078-9)
9. C. N. Maréchal, P. Télouk, and F. Albarède, *Chem. Geol.*, 1999, **156**, 251-273. [https://doi.org/10.1016/S0009-2541\(98\)00191-0](https://doi.org/10.1016/S0009-2541(98)00191-0)
10. J. Li, S.-h. Tang, X.-k. Zhu, Z.-h. Li, S.-Z. Li, B. Yan, Y. Wang, J. Sun, Y. Shi, A. Dong, N. S. Belshaw, X. Zhang, S.-a. Liu, J.-h. Liu, D. Wang, S.-y. Jiang, K. Hou, and A. S. Cohen, *Geostand. Geoanal. Res.*, 2019, **43**, 163-175. <https://doi.org/10.1111/ggr.12241>
11. M. Zhao, L. G. Tarhan, Y. Zhang, A. Hood, D. Asael, R. P. Reid, and N. J. Planavsky, *Earth Planet. Sc. Lett.*, 2021, **553**, 116599. <https://doi.org/10.1016/j.epsl.2020.116599>
12. J. B. Chapman, T. F. D. Mason, D. J. Weiss, B. J. Coles, and J. J. Wilkinson, *Geostand. Geoanal. Res.*, 2006, **30**, 5-16. <https://doi.org/10.1111/j.1751-908X.2006.tb00907.x>
13. A. E. Shiel, J. Barling, K. J. Orians, and D. Weis, *Anal. Chim. Acta*, 2009, **633**, 29-37. <https://doi.org/10.1016/j.aca.2008.11.026>
14. P. A. Sossi, G. P. Halverson, O. Nebel, and S. M. Eggins, *Geostand. Geoanal. Res.*, 2015, **39**, 129-149. <https://doi.org/10.1111/j.1751-908X.2014.00298.x>
15. S. Chen, Y. Liu, J. Hu, Z. Zhang, Z. Hou, F. Huang, and H. Yu, *Geostand. Geoanal. Res.*, 2016, **40**, 417-432. <https://doi.org/10.1111/j.1751-908X.2015.00377.x>
16. K. Moeller, R. Schoenberg, R.-B. Pedersen, D. Weiss, and S. Dong, *Geostand. Geoanal. Res.*, 2012, **36**, 177-199. <https://doi.org/10.1111/j.1751-908X.2011.00153.x>
17. A. Makishima and E. Nakamura, *J. Anal. At. Spectrom.*, 2013, **28**, 127-133. <https://doi.org/10.1039/C2JA30271C>

18. Q. Amet and C. Fitoussi, *Inter. J. Mass Spectrom.*, 2020, **457**, 116413. <https://doi.org/10.1016/j.ijms.2020.116413>
19. M. Druce, C. H. Stirling, and J. M. Rolison, *Geostand. Geoanal. Res.*, 2020, **44**, 711-732. <https://doi.org/10.1111/ggr.12341>
20. C. Rosca, S. König, M.-L. Pons, and R. Schoenberg, *Chem. Geol.*, 2021, **586**, 120440. <https://doi.org/10.1016/j.chemgeo.2021.120440>
21. C. Archer and D. Vance, *J. Anal. At. Spectrom.*, 2004, **19**, 656-665. <https://doi.org/10.1039/B315853E>
22. F. Lamer, M. Rehkämper, B. J. Coles, K. Kreissig, D. J. Weiss, B. Sampson, C. Unsworth, and S. Strelkopytov, *J. Anal. At. Spectrom.*, 2011, **26**, 1627-1632. <https://doi.org/10.1039/C1JA10067J>
23. S.-A. Liu, D. Li, S. Li, F.-Z. Teng, S. Ke, Y. He, and Y. Lu, *J. Anal. At. Spectrom.*, 2014, **29**, 122-133. <https://doi.org/10.1039/C3JA50232E>
24. H.-Y. Zhai, X.-C. Wang, C.-F. Li, S. A. Wilde, X.-Z. Li, B. Xu, X.-L. Zhang, and P. Zhang, *RSC Adv.*, 2023, **13**, 19030-19038. <https://doi.org/10.1039/D3RA00603D>
25. W. Lian, F. Ren, L. Tang, and D. Dong, *Microchem. J.*, 2016, **129**, 194-199. <https://doi.org/10.1016/j.microc.2016.06.021>
26. Z. Bao, K. Huang, T. Huang, B. Shen, C. Zong, K. Chen, and H. Yuan, *J. Anal. At. Spectrom.*, 2019, **34**, 940-953. <https://doi.org/10.1039/C9JA00002J>
27. W.-G. Liu, S. Wei, J. Zhang, C. Ao, F.-T. Liu, B. Cai, H.-Y. Zhou, J.-L. Yang, and C.-F. Li, *J. Anal. At. Spectrom.*, 2020, **35**, 953-960. <https://doi.org/10.1039/D0JA00035C>
28. J. Wang, D.-M. Tang, Q.-H. Yuan, B.-X. Su, W.-J. Li, B.-Y. Gao, Z.-A. Bao, and Y. Zhao, *Geostand. Geoanal. Res.*, 2023, **47**, 969-982. <https://doi.org/10.1111/ggr.12499>
29. Y. Yang, X. Zhang, S.-A. Liu, T. Zhou, H. Fan, H. Yu, W. Cheng, and F. Huang, *J. Anal. At. Spectrom.*, 2018, **33**, 1777-1783. <https://doi.org/10.1039/C8JA00249E>
30. S. G. John, J. Genevieve Park, Z. Zhang, and E. A. Boyle, *Chem. Geol.*, 2007, **245**, 61-69. <https://doi.org/10.1016/j.chemgeo.2007.07.024>
31. H. Yuan, W. Yuan, Z. Bao, K. Chen, F. Huang, and S. Liu, *Geostand. Geoanal. Res.*, 2017, **41**, 77-84. <https://doi.org/10.1111/ggr.12127>
32. T. F. D. Mason, D. J. Weiss, M. Horstwood, R. R. Parrish, S. S. Russell, E. Mullane, and B. J. Coles, *J. Anal. At. Spectrom.*, 2004, **19**, 209-217. <https://doi.org/10.1039/B306958C>
33. X. Nie, Z. Bao, P. Liang, K. Chen, C. Zong, and H. Yuan, *Atom. Spectrosc.*, 2022, **43**, 117-125. <https://doi.org/10.46770/as.2021.910>
34. Y. Han, L. Zhou, M. Shi, Y. Hu, G. Zhang, X. Hou, and L. Feng, *J. Anal. At. Spectrom.*, 2024, **39**, 269-280. <https://doi.org/10.1039/D3JA00298E>
35. Y. Lv, S.-A. Liu, J.-M. Zhu, and S. Li, *Chem. Geol.*, 2016, **445**, 24-35. <https://doi.org/10.1016/j.chemgeo.2016.01.016>
36. Z.-Z. Wang, S.-A. Liu, Z.-C. Liu, Y.-C. Zheng, and F.-Y. Wu, *Geochim. Cosmochim. Acta*, 2020, **278**, 305-321. <https://doi.org/10.1016/j.gca.2019.09.026>
37. J. Huang, X.-C. Zhang, S. Chen, L. Tang, G. Wörner, H. Yu, and F. Huang, *Geochim. Cosmochim. Acta*, 2018, **238**, 85-101. <https://doi.org/10.1016/j.gca.2018.07.012>
38. E. D. Young, A. Galy, and H. Nagahara, *Geochim. Cosmochim. Acta*, 2002, **66**, 1095-1104. [https://doi.org/10.1016/S0016-7037\(01\)00832-8](https://doi.org/10.1016/S0016-7037(01)00832-8)
39. L. S. Doucet, O. Laurent, N. Mattielli, and W. Debouge, *Chem. Geol.*, 2018, **476**, 260-271. <https://doi.org/10.1016/j.chemgeo.2017.11.022>